1986

Predictions of Heat Transfer in Compressor Cylinders

G. W. Recktenwald

J. W. Ramsey

S. V. Patankar

PREDICTIONS OF HEAT TRANSFER IN COMPRESSOR CYLINDERS

Gerald W. Recktenwald, Research Assistant
James W. Ramsey, Associate Professor
Suhas V. Patankar, Professor

Mechanical Engineering Department
University of Minnesota
111 Church St. SE
Minneapolis, MN 55455

ABSTRACT

Two numerical models are used to investigate the instantaneous heat transfer between the cylinder walls and gas in a reciprocating compressor. One model uses simple mass and energy balances to predict the bulk thermodynamic properties of the gas in the cylinder. Heat transfer between the cylinder walls and the gas is calculated with a widely used correlation for the heat transfer coeffiecient. The other model solves the unsteady continuity, momentum, and energy equations for the gas in the cylinder using a finite-difference technique. No heat transfer coefficient is needed in this model. Results from the finite-difference model agree quite well with the published results from experiments and similar computations for compressors and non-firing reciprocating engines. The instantaneous heat transfer predicted by the simple model is an order of magnitude less than that predicted by the finite-difference model.

INTRODUCTION

Heat transfer between the cylinder walls and the gas affects the thermal efficiency of reciprocating compressors. The significance of heat transfer has been debated [1, 2, 3], but no definitive answers have been offered for two questions. How important is heat transfer in determining compressor efficiency, and to what extent can designers control the impact of heat transfer?

Research on the effect of heat transfer has taken two basic approaches. The first combines experimental measurements with a heat balance to determine the overall heat transferred to the gas [4, 5, 6, 7]. The advantage of this approach is that it is straightforward. The main disadvantage is that it gives compressor designers little insight into the mechanisms of heat transfer, and the design changes that can improve compressor performance.

The second approach uses a numerical model based on the first law of thermodynamics [2, 8, 9]. An advantage of this approach is that parameters may easily be changed to predict the effects of design modifications. The chief disadvantages

are that these models may not adequately simulate compressor performance, and ultimately these models depend on an experimentally determined correlation for the heat transfer coefficient.

The work described in this report uses a third approach. The basic differential equations describing the flow and heat transfer of the gas in the cylinder space are solved using a finite-difference technique [10]. This method was first applied to piston cylinder configurations by Gosman and Watkins [11]. Their technique has been developed further and applied to the geometry of a reciprocating compressor.

The finite-difference model is called the multinode model because the state properties of the gas are calculated at many nodes inside the cylinder. Earlier reasearch [9] lead to the development of the so-called three node model; the three nodes are the suction plenum, the cylinder space, and the discharge plenum. The multinode model essentially replaces the single node corresponding to the cylinder space with a finite-difference grid.

THE THREE NODE MODEL

The three node model is similar in many respects to other models used to simulate compressors. Our derivation of the energy equation follows that given by Karll [13]. The gas in the cylinder is assumed to have a uniform pressure and temperature. Valve dynamic calculations are included to account for the instantaneous changes in port area. Gas flow to and from the cylinder is controlled by the size of the valve openings and the pressure difference across the ports. Pulsations in the suction and discharge plenums are not calculated but could be prescribed functions of time. In the present work the plenum pressures are assumed to be constant. The emphasis of the three node model is on the processes that most immediately affect the state of the gas in the cylinder. The three node model is, therefore, not a complete compressor simulation.

The following derivation of the energy equation for the gas in the cylinder will help to illuminate the essential features of the model. A general form of the energy equation for an open system is [14]:

$$\frac{dE}{dt} = \dot{Q} + \dot{W} + (e + p\hat{v})_{in}\dot{m}_{in} - (e + p\hat{v})_{out}\dot{m}_{out} \tag{1}$$

where dE/dt is the time rate of increase of the total energy of the gas in the cylinder, $\dot{Q}$ is rate at which heat is added to the gas, $\dot{W}$ is the rate at which work is done on the gas, $\dot{m}_{in}$ and $\dot{m}_{out}$ are the rates at which the gas is entering and leaving the cylinder, respectively, e is the specific energy of the gas, p is the pressure, and $\hat{v}$ is the specific volume. Neglecting changes in gravitational and kinetic energy

$$\frac{dE}{dt} = \frac{d}{dt}(mu) = u(\dot{m}_{in} - \dot{m}_{out}) + m\frac{du}{dt}$$

where u is the specific internal energy of the gas, and m is the mass in the cylinder.

The mass flow rates $\dot{m}_{in}$ and $\dot{m}_{out}$ are determined by submodels of the gas flow through the ports. The gas flow is assumed to be governed by the one dimensional isentropic equations describing the flow of gas from a quiescent reservoir [15]. The flow area is determined by a function relating the flow area to the valve lift [16]. The valve lift is found by integrating the second order dynamical equations governing the motion of the valves.

Using standard thermodynamic manipulations [14] the rate of change of specific internal energy may be written as

$$\frac{du}{dt} = c_v \frac{dT}{dt} + \left[T\left(\frac{\partial p}{\partial T}\right)_{\hat{v}} - p\right]\frac{d\hat{v}}{dt}$$

and from the definition $\hat{v} \equiv V/m$ where V is the instantaneous cylinder volume we have

$$\frac{d\hat{v}}{dt} = \frac{1}{m}\frac{dV}{dt} - \frac{V}{m^2}\frac{dm}{dt}$$

The rates of heat transfer to the gas and work done on the gas are, respectively,

$$\dot{Q} = \overline{h}_c A_s (T_w - T_b)$$

$$\dot{W} = p\frac{dV}{dt}$$

where $\overline{h}_c$ is the heat transfer coefficient between the cylinder wall and the gas, A_s is the instantaneous surface area of the cylinder walls, T_w is the wall temperature, T_b is the bulk temperature of the gas.

Substituting the above equations into equation (1) yeilds an equation of the form

$$\frac{dT_b}{dt} = A(t) + B(t)T_b \tag{2}$$

The terms $A(t)$ and $B(t)$ will depend on the equation of state used to describe the gas. For an ideal gas,

$$A(t) = \frac{1}{mc_v}\left[\overline{h}_c A_s T_w + \dot{m}_{in} h_{in}\right]$$

$$B(t) = \frac{\overline{h}_c A_s}{mc_v} + \frac{\gamma - 1}{V}\frac{dV}{dt} + (\gamma - 1)\frac{\dot{m}_{out}}{m} + \frac{\dot{m}_{in}}{m}$$

where h_{in} is the enthalpy of the gas entering the cylinder from either the suction plenum for normal flow or the discharge plenum for backflow.

Equation (2) may now be written in implicit finite-difference form as

$$\frac{T_b - T_b^o}{\Delta t} = A(t) + B(t)T_b \tag{3}$$

where T_b, $A(t)$, and $B(t)$ are all values at the new time t. The implicit formulation is used because it is unconditionally stable, and it is also convenient.

Equation (3) is integrated by successive substitution until the bulk temperature has converged to within 0.5 °C (~0.3 °F). If convergence is not obtained within six time steps, the time step Δt is halved. An additional constraint is imposed to guarantee that the step size is not too large during the suction and discharge processes. If the relative change in mass is greater than 10% during any one time step the time step is also cut in half. The integration is continued until a cycle (one

crank rotation) is completed. At that time cycle totals are calculated. After six cycles are completed the cycle totals and the instantaneous pressure and temperature variations are observed to repeat, and the model is said to have converged.

THE FINITE-DIFFERENCE MODEL

It is impossible to present all the details of the multinode model in the available space; only the most essential equations will be presented here. Interested readers should consult references [17] and [10] for a complete description.

The calculation domain for the multinode model is shown in Figure 1. The two-dimensional, axisymmetric domain is bounded by the cylinder head, the cylinder wall, the piston face and the centerline of the cylinder. Figure 1 is not drawn to scale, also the grid drawn in the Figure is not the actual grid used in the calculations. Gas enters through the suction port and leaves through the discharge port. No backflow is allowed in the multinode model. The gas gains or loses heat by convection to the cylinder head, the cylinder wall, and the piston. No mass or energy is transported across the axis of symmetry.

The domain is divided into three regions labelled 1, 2 and 3. Region 1 contains the clearance volume, region 2 is the space between the clearance volume and the suction valve, and region 3 is the space between the suction valve and the piston face. Each of these regions is delineated by grid lines that are either fixed or are a prescribed function of time. The grid line on the boundary between regions 1 and 2 moves with the suction valve. When the suction valve is closed the grid in region 2 is collapsed into a negligibly small space. The location of the grid line that moves with the suction valve is determined by the output of the three node model. The location of the piston face is obtained from the kinematics of the slider crank mechanism.

The Conservation Equations

The multinode finite-difference model obtains solutions to the differential equations governing mass, momentum, and energy conservation for the gas. The conservation of mass is expressed by the continuity equation

$$\frac{\partial \rho}{\partial t} + \frac{\partial}{\partial x}(\rho u) + \frac{1}{r}\frac{\partial}{\partial r}(\rho r v) = 0$$

The unsteady Navier-Stokes equations and the energy equation may be put in the form of a general ϕ equation [10]

$$\frac{\partial}{\partial t}(\rho\phi) + \frac{\partial}{\partial x}(\rho u\phi) + \frac{1}{r}\frac{\partial}{\partial r}(\rho r v\phi) = \frac{\partial}{\partial x}\left[\Gamma_\phi \frac{\partial \phi}{\partial x}\right] + \frac{1}{r}\frac{\partial}{\partial r}\left[r\Gamma_\phi \frac{\partial \phi}{\partial r}\right] + S_\phi$$

where ϕ is a scalar, Γ_ϕ is the diffusion coefficient for the transport of ϕ, and S_ϕ is the source term. By choosing particular values from Table 1 the general ϕ equation can be used to represent one of the three conservation equations. For example, when $\phi = u$, $\Gamma_\phi = \mu_t$, and $S_\phi = -\partial p/\partial x$ the general ϕ equation becomes the x–direction momentum equation.

The multinode model incorporates a highly simplified turbulence model. Turbulent flow is characterized by a large effective viscosity due to enhanced mixing caused by turbulent eddies. We define a turbulence Reynolds number $Re_t \equiv \rho U D/\mu_t$ where

Equation	ϕ	Γ_ϕ	S_ϕ
x-direction momentum	u	μ_t	$-\frac{\partial p}{\partial x}$
r-direction momentum	v	μ_t	$-\frac{\partial p}{\partial r} - \frac{\mu u}{r^2}$
energy	h	μ_t	$\frac{dp}{dt}$

Table 1. Scalar quantities associated with the general ϕ equation.

U is the mean piston speed, D is the cylinder bore, and μ_t is the turbulence viscosity. In many practical situations $Re_t \sim 100 - 500$. In the present work a value of $Re_t = 250$ is chosen and the value of μ_t is obtained from the definition of Re_t. (A sensitivity analysis has determined that the trends of the results presented here are virtually independent of Re_t.) By invoking the Reynolds analogy [18] the diffusion coefficient Γ_h for the transport of enthalpy is also μ_t as is shown in Table 1.

In the results presented here the gas is assumed to be an ideal gas. The above conservation equations apply to all gases that are Newtonian fluids. Extension of the multinode model to a real gas equation of state is possible at the expense of added complication to the global pressure and temperature correction algorithm discussed below.

The Moving Grid

To solve the conservation equations inside the cylinder space the general ϕ equation is transformed from the inertial coordinate system (x, r, t) to the moving coordinate system (ξ, r, t). Each grid line has a unique value of ξ which does not change with time. Hence the boundaries between the regions described above may be identified by particular values of ξ. The general ϕ equation may be transformed to the (ξ, r, t) coordinate system with

$$\frac{x - x_1}{x_2 - x_1} = \frac{\xi - \xi_1}{\xi_2 - \xi_1}$$

where ξ_1, ξ_2, x_1, and x_2 are the coordinates of the boundaries of the grid regions. Using this transformation the continuity equation becomes

$$\frac{1}{L}\frac{\partial}{\partial t}(\rho L) + \frac{1}{L}\frac{\partial}{\partial \xi}(\rho \tilde{u}) + \frac{1}{r}\frac{\partial}{\partial r}(\rho r v) = 0 \tag{4}$$

The general ϕ equation transforms to

$$\frac{1}{L}\frac{\partial}{\partial t}(L\rho\phi) + \frac{1}{L}\frac{\partial}{\partial \xi}(\rho\tilde{u}\phi) + \frac{1}{r}\frac{\partial}{\partial r}(\rho r v \phi) = \frac{1}{L}\frac{\partial}{\partial \xi}\left[\frac{\Gamma_\phi}{L}\frac{\partial \phi}{\partial \xi}\right] + \frac{1}{r}\frac{\partial}{\partial r}\left[r\Gamma_\phi \frac{\partial \phi}{\partial r}\right] + \tilde{S}_\phi \tag{5}$$

where $L \equiv (\partial x/\partial \xi)_t$ is a length scale, and $\tilde{S}_\phi$ is the source term transformed to the (ξ, r, t) system, $\tilde{u}$ is the velocity of the fluid relative to the grid, and u_g is the local grid velocity

$$\tilde{u} \equiv u - u_g$$

$$u_g \equiv \left(\frac{\partial x}{\partial t}\right)_\xi$$

Global Pressure and Temperature Correction

The transformed equations are very similar to the original equations. This enables us to use finite-difference techniques developed for fixed grids with suitable modifications. The system of equations (4) and (5) are solved with the pressure-velocity coupling algorithm called SIMPLER [10].

Compression and expansion of the gas causes large changes in the bulk pressure and temperature. These changes are evident in the equation of state and as a source term in the energy equation (cf. Table 1). A global pressure and temperature correction algorithm [11,12,17], which enhances the convergence by anticipating these changes, is incorporated into the solution procedure.

Changing the volume of the calculation domain alters the local density and local enthalpy. This requires an iterative procedure to adjust the current density and enthalpy until it reflects the conditions at the new cylinder volume. If the current, or guessed, values of local density and enthalpy are denoted by ρ^* and h^*, while the ultimate, or correct, values are denoted by ρ and h, then

$$\rho = \rho^* + \Delta\rho \tag{6a}$$

$$h = h^* + \Delta h \tag{6b}$$

These local changes are related to the global changes, or corrections, $\Delta\overline{p}$ and $\Delta\overline{T}$ by

$$\Delta\rho = \left(\frac{\partial\rho}{\partial p}\right)_T \Delta\overline{p} + \left(\frac{\partial\rho}{\partial T}\right)_p \Delta\overline{T} \tag{7a}$$

$$\Delta h = \left(\frac{\partial h}{\partial p}\right)_T \Delta\overline{p} + \left(\frac{\partial h}{\partial p}\right)_p \Delta\overline{T} \tag{7b}$$

Now, the expansions in equations (7a) and (7b) are substituted into equations (6a) and (6b). The results are then substituted into the transformed continuity equation (4) and the transformed energy equation (use equation (5) with $\phi = h$) and integrated over the calculation domain. Neglecting second and third order corrections, e.g. $\Delta\rho\Delta h$, one obtains a system of two linear, simultaneous equations for $\Delta\overline{p}$ and $\Delta\overline{T}$ that may be solved algebraically.

Boundary Conditions

The boundary conditions for the axisymmetric computational domain sketched in Figure 1 are as follows. The absolute velocities on all fixed surfaces are zero. The axial velocity on the piston face is equal to the instantaneous piston velocity. The

temperature at the wall is a constant equal to the average of the suction and discharge temperatures. All dependent quantities are symmetrical about the centerline.

The inflow and outflow boundary conditions pose some unique problems to the multinode model. The gas flow across the boundaries depends on the state of the gas in the cylinder while calculation of the velocity and enthalpy fields inside the cylinder requires prescribed values of the velocity and enthalpy (temperature) at all boundaries.

The problem of specifying the inflow boundary condition is solved by using the output of the three node model as input to the multinode model. The instantaneous suction gas velocity calculated by the three node model defines the inflow velocity for the multinode model. The data is adjusted so that there is no backflow (which is allowed by the three node model) and the total mass flow per cycle is the same for both models.

Given the instantaneous inflow velocity and the instantaneous lift of the suction and discharge valves, the multinode model calculates the velocity and enthalpy fields. This may at first seem like an artificial problem: if the mass flow to the cylinder is prescribed what can be gained by calculating the velocity and enthalpy fields inside the cylinder? Such a calculation procedure, however, yields a very important result, namely, the local heat transfer between the cylinder wall and the gas.

The multinode model does not need a heat transfer correlation since the local heat transfer rate is obtained directly from the temperature gradient of the gas adjacent to the solid boundaries. Integration of the local heat transfer rate over the surface area of the solid boundaries yields the total heat transfer rate to the gas at each time step. The three node model uses a correlation [19] to calculate this heat transfer rate. Thus, the multinode model may be used to check the validity of the heat transfer correlation used in the three node model.

RESULTS

Results are presented for a single run for each of the two models. The gas is Refrigerant 12, and all thermophysical properties are evaluated at the average of the suction and discharge temperatures. In both models the properties are assumed to be constant and uniform throught the cylinder space. The simulated operating conditions are a suction pressure of 0.384 MPa (55.7 psia) and a discharge pressure of 1.423 MPa (206.4 psia). These pressures correspond to saturated evaporating and condensing temperatures of 280 °K (45 °F) and 330 °K (134 °F) respectively. The temperature of the gas entering the cylinder is 325 °K (125 °F). The large superheating of the suction gas above its saturated evaporating temperature is an attempt to account for heat transfer to the gas *before* it enters the compressor cylinder. The cylinder wall temperature is 354 °K (177 °F) (average temperature of the gas entering and leaving the cylinder).

The compressor bore is 63.5 mm (2.5 in) and the stroke is 50.8 mm (2.0 in). The clearance volume is 7% of the total cylinder volume and the compressor speed is 1750 RPM. The computations for the multinode model are carried out on an 18 x 19 grid. Convergence is obtained in 6 cycles when 90 time steps per cycle are taken. The three node model converges in 7 cycles with 211 time steps per cycle.

Flow Field Predictions

The velocity field in the compressor cylinder is represented by the plots in Figure 2. These consist of 6 plot frames chosen from the 90 time steps that constitute

a complete compressor cycle. Each plot frame can be interpreted as a snapshot of the flow pattern at a given crank angle. The crank angle θ is 0 at top dead center (TDC) and increases to 180 degrees during the suction process. During compression θ varies from 180 to 360 degrees. The arrows in Figure 2 represent the velocity vectors calculated by the multinode model. Arrows along the bottom boundary of each plot frame indicate the direction and magnitude of the piston velocity.

The dominant feature of the flow field for most of the frames is a toroidal vortex, rotating in the counterclockwise direction. The vortex is driven by the annular jet of gas entering through the suction valve. The suction valve opens at $\theta = 45$. It remains open in the second ($\theta = 93$) and third ($\theta = 167$) plot frames. The suction jet spreads and is drawn toward the piston where it is deflected outward toward the cylinder wall.

The fourth and fifth plot frames in Figure 2 ($\theta = 206$) and ($\theta = 279$) show the flow field during the compression process. The toroidal vortex is compressed, and its center moves toward the centerline of the cylinder. The largest velocities appear along a radial line between the suction valve and the centerline. This is the region of the grid that is compressed by the closing of the suction valve.

The discharge valve opens at $\theta = 311$. The last plot frame in Figure 2 depicts the flow field during the discharge process. The three arrows crossing the left boundary show the velocity of the gas leaving the domain. As in the previous two frames there is a large, radial velocity component for the control volumes aligned with the suction valve. These large velocities persist even after the piston moves through TDC and begins to expand the gas left in the clearance space—see the plot frame for $\theta = 43$.

The unrealistically large velocities in the plane of the suction valve are the result of grid distortion caused when region 2 of the grid (cf. Figure 1) collapses into an extremely narrow space. The rest of the flow field is qualitatively realistic. Although these large velocities distort the flow field they do not significantly affect the other results of the multinode model.

Variation of Bulk Quantities

Since the three node model does not compute local velocities and enthalpies the only means of comparison between the two models is on the basis of bulk quantities. Figures 3 and 4 represent the variation of the mean cylinder pressure and bulk temperature with crank angle θ.

The pressure histories predicted by the two models are in good agreement except during the discharge process. This discrepancy could be reduced by adjusting a flow area parameter that describes the discharge process. The temperature histories of the two models are at great variance with each other. The three node model predicts higher temperatures during the discharge and expansion processes while the multinode model predicts higher temperatures during suction and compression.

Table 2 is a summary of the cycle totals for the two models. The total mass flow for the two models is identical, as is intended in this analysis. The required input power is the cyclic integral of the $p\,dV$ work for a single cylinder divided by the time to complete a cycle. Friction losses, manifold pressure drops, and other losses are not considered. As shown in Table 2 the power requirement calculated by the multinode model is 8% greater than that calculated by the three node model. The discrepancy is due to the difference in instantaneous pressure calculated by the two models as Figure 3 indicates.

The average, net heat transfer rate is the net heat transferred to the gas in one cycle divided by the time required to complete a cycle. Since the heat transfer is both positive and negative during a cycle, the difference in the predicted net heat transfer rate is considerably less than the difference in the predicted instantaneous heat transfer rate. The net heat transfer rate predicted by the multinode model is 132% greater than that predicted by the three node model.

	Three node model	Multinode model	difference*
total mass flow, $\frac{kg}{cycle}$	2.26×10^{-3}	2.26×10^{-3}	0
required input power	2360 W	2340 W	+8%
average net heat transfer to the gas	72 W	167 W	+132%
discharge temperature	383 K	367 K	−4%

Table 2. Comparison of cycle totals for the two models

*difference relative to the multinode model

Instantaneous Heat Transfer Rates

The discrepancy between the temperature histories is a reflection of the striking disagreement in the calculated heat transfer rates, which is depicted in Figure 5. During compression the peak heat transfer rate predicted by the multinode model is -6850 W, (heat transfer is negative when heat is removed from the gas) compared to -150 W predicted by the three node model. During suction the multinode model predicts a peak heat transfer rate of 3340 W, and the three node model predicts 340 W.

The heat transfer rate calculated by the three node model is so small in comparison to that calculated by the multinode model that the compressor appears to be adiabatic. It is not surprising then that researchers [2] using the correlation of Adair et al. [19] have concluded that the modeling of heat transfer in reciprocating compressors is not important. A more recent correlation [20] predicts heat transfer rates that are much larger than that predicted by the Adair correlation.

Upon first inspection of Figure 5 the reader may be skeptical of the computer programs used to generate those results. It does not seem plausible that two well conceived models could predict heat transfer rates that differ by as much as an order of magnitude. To check the results of the two models literature on heat transfer in compressors and motored, i.e. non-firing, engines was consulted.

Other researchers [12, 21, 22] have used finite-difference techniques to calculate the flow field and heat transfer inside compressor and motored engine cylinders. For comparable operating conditions peak heat transfer rates of up to 100 kW [21] have been reported. This is even an order of magnitude larger than the predictions of the multinode model. Similar models [21, 22] have predicted peak heat transfer rates on the order of 10 kW. These latter results are in good agreement with the multinode model, for which the magnitude of the peak heat transfer rate is approximately 7 kW.

Measurements of the local heat flux in motored engines have been reported by several researchers, e.g. [23, 24, 25]. The experiments on engines were made with air as the working fluid with the intake at atmospheric conditions. Air has a Prandtl number ($Pr = \mu c_p/k$) of 0.7, compared to 0.8 for Refrigerant 12. Although an exact comparison cannot be made between engines and compressors, by examining the magnitude of the measured wall heat flux one can determine whether the results of the multinode model are realistic.

In the experiments cited above peak heat flux values between $-800\,\mathrm{kW/m^2}$ and $100\,\mathrm{kW/m^2}$ were observed. These compare favorably with the range $-600\,\mathrm{kW/m^2}$ to $400\,\mathrm{kW/m^2}$ calculated by the multinode model. The results of the multinode model, therefore, appear to be realistic when compared to heat transfer experiments on engines and compressors. The agreement with other finite-difference models also lends credibility to the predictions of the multinode model.

CONCLUSIONS

Results of the multinode model agree quite well with the published results from experiments and similar computations for compressors and non-firing reciprocating engines. Continued research is aimed at incorporating a more sophisticated turbulence model, extending the computations to finer grids, and removing the effects of local grid distortion. Despite its present limitations the multinode model predicts instantaneous heat transfer rates consistent with results of comparable research.

The three node model uses a heat transfer correlation widely used in simulations of reciprocating compressors. From the results of this model one might conclude that reciprocating compressors are nearly adiabatic. This conclusion, however, is contrary to the predictions of the multinode model and results published in the open literature.

The results of the multinode model cast considerable doubt on the validity of the heat transfer correlation obtained by Adair et al. Any analysis based on this correlation is also dubious.

ACKNOWLEDGEMENTS

This work was supported by Carlyle Compressor Division of United Technologies Corporation, and the University of Minnesota Academic Computing Services and Systems.

REFERENCES

1. Qvale, E. B., Soedel, W., Stevenson, M. J., Elson, J. P., and Coates, D. A., " Problem areas in mathematical modeling and simulation of refrigerating compressors", *1972 ASHRAE Transactions*, paper no. 2215
2. Brok, S. W., Touber, S., van der Meer, J. S., "Modeling of cylinder heat transfer —large effort, little effect?",*Proceedings of the 1980 Purdue Compressor Technology Conference*, Purdue University, West Lafayette, IN.
3. Lee, K., and Smith, J. L. Jr., "Time resolved mass flow measurement for a reciprocating compressor", *Proceedings of the 1980 Purdue Compressor Technology Conference*, Purdue University, West Lafayette, IN.
4. Lee, K., and Smith, J. L. Jr., "Influence of cyclic wall-to-gas heat transfer in the cylinder of the valved hot-gas engine", *Proceedings of the* 13^{th} *Intersociety Energy Conversion Conference*, San Diego, CA, 1978, SAE paper no. 789195.

5. Lee, K., and Smith J. L. Jr., "Performance loss due to transient heat transfer in the cylinders of stirling engines", *Proceedings of the* 15^{th} *Intersociety Energy Conversion Conference*, Seattle, WA, 1980, AIAA paper no. 809338.

6. Woschni, G., "A universally applicable equation for the instantaneous heat transfer coefficient in the internal combustion engine", *1967 SAE Transactions*, paper no. 670931.

7. Nishiwake, K., Shimamoto, Y., and Miyaka, K., "Average heat transfer coefficients on a cylinder wall in the intake and exhaust processes of motoring test", *Bul. JSME*, **22**(174), December 1979.

8. Lee, S., Singh, R., and Moran, M. J., "First law analysis of a compressor using a computer simulation model", *Proceedings of the 1982 Purdue Compressor Technology Conference*, Purdue University, West Lafayette, IN.

9. Recktenwald, G. W., "A simulation of a reciprocating compressor based on instantaneous energy and mass conservation", *Environmental Division Technical Report*, University of Minnesota Dept. of Mech. Eng., October 1982, Minneapolis, MN.

10. Patankar, S. V., *Numerical Heat Transfer and Fluid Flow*, 1980 McGraw-Hill.

11. Gosman, A. D., and Watkins, A. P., "A computer prediction method for turbulent flow and heat transfer in piston/cylinder assemblies", *Proceedings of the Symposium on Turbulent Shear Flows*, Vol. I, April 18-20, 1977, Pennsylvania State University, University Park, PA.

12. Gosman, A. D., and Watkins, A. P., "Predictions of local instantaneous heat transfer in idealized motored reciprocating engines", *Mechanical Engineering Department Technical Report FS/79/28*, Imperial College of Science and Technology, London, UK.

13. Karll, B., "Computer simulation of the cylinder process in a compressor based on the first law of thermodynamics", *Proceedings of the 1972 Purdue Compressor Technology Conference*, Purdue University, West Lafayette, IN.

14. Wark, K., *Thermodynamics*, 1977 McGraw-Hill.

15. Shapiro, A., *The Dynamics and Thermodynamics of Compressible Fluid Flow*, 1953 Wiley and Sons.

16. Schwerzler, D. D., and Hamilton, J. F., "An analytical method for determining effective flow and force areas for refrigeration compressor valving systems", *Proceedings of the 1972 Purdue Compressor Technology Conference*, Purdue University, West Lafayette, IN.

17. Recktenwald, G. W., *Numerical Modeling of the Flow and Heat Transfer in the Cylinder of a Reciprocating Compressor*, MS Thesis, University of Minnesota Department of Mechanical Engineering, Minneapolis, MN.

18. Kays, W. M., and Crawford, M. E., *Convective Heat and Mass Transfer*, 1980 McGraw-Hill.

19. Adair, R. P., Qvale, E. B., and Pearson, J. T., "Instantaneous heat transfer to the cylinder wall in a reciprocating compressor", *Proceedings of the 1972 Purdue Compressor Technology Conference*, Purdue University, West Lafayette, IN.

20. Liu, R. and Zhou, Z., "Heat transfer between gas and cylinder wall of refrigerating reciprocating compressor", *Proceedings of the 1984 International Compressor Engineering Conference*, Purdue University, West Lafayette, IN.

21. Chong, M. S., and Watson, H. C., "Prediction of heat and mass transfer during compression in reciprocating compressors", *Proceedings of the 1976 Purdue Compressor Technology Conference*, Purdue University, West Lafayette, IN.

22. Ramos, J. I., and Sirignano, W. A., "Axisymmetric, unsteady calculations in a piston-cylinder configuration", *Proceedings of the 1979 National Conference on Numerical Methods in Heat Transfer*, University of Maryland, College Park, MD.

23. Overbye, V. D., Bennethum, J. E., Uyehara, O. A., Meyers, P. S., "Unsteady heat transfer in engines", *1961 SAE Transactions*, vol. 69, pp. 461-494.

24. Annand, W. J. D., and Pinfold, D., "Heat transfer in the cylinder of a reciprocating engine", *1980 SAE Transactions*, SAE paper no. 800457.

25. Alkidas, A. C., "Heat transfer characteristics of a spark ignition engine", *Journal of Heat Transfer*, vol. 102, May 1980.

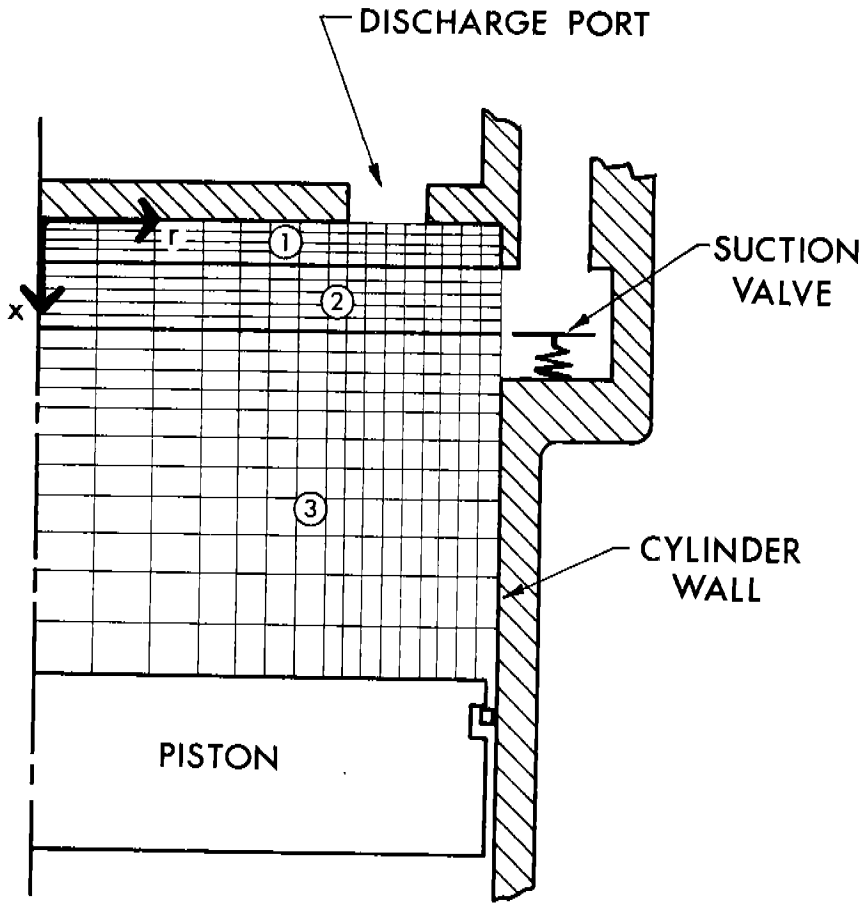

Figure 1. Calculation domain for the multinode model.

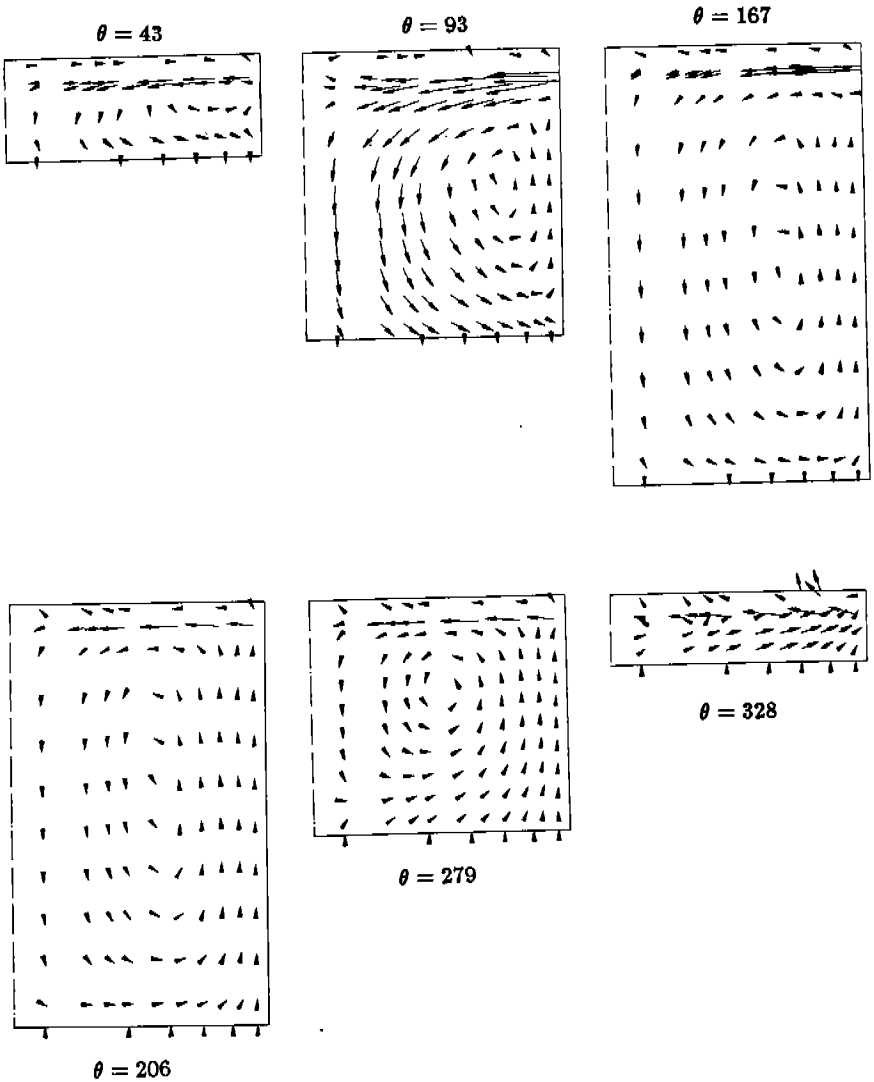

Figure 2. Velocity fields in the compressor cylinder.

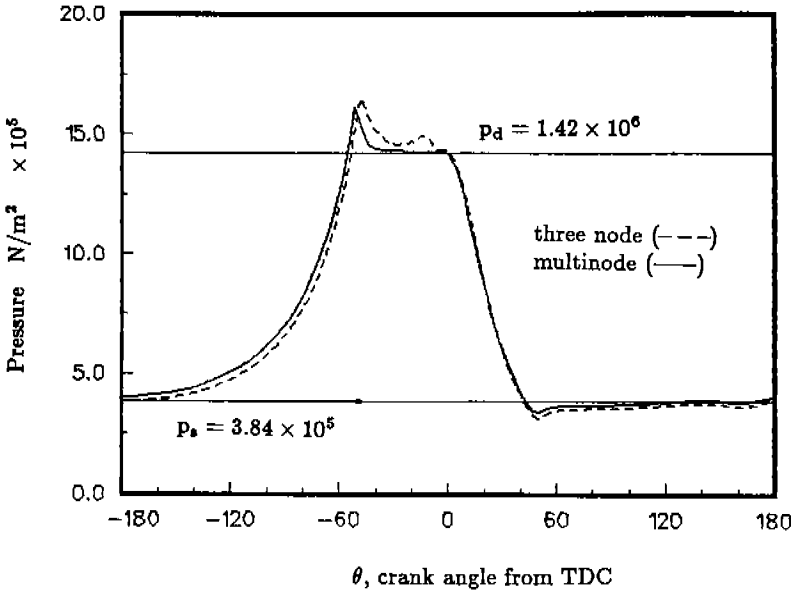

Figure 3. Comparison of instantaneous pressures calculated by the three node and multinode models.

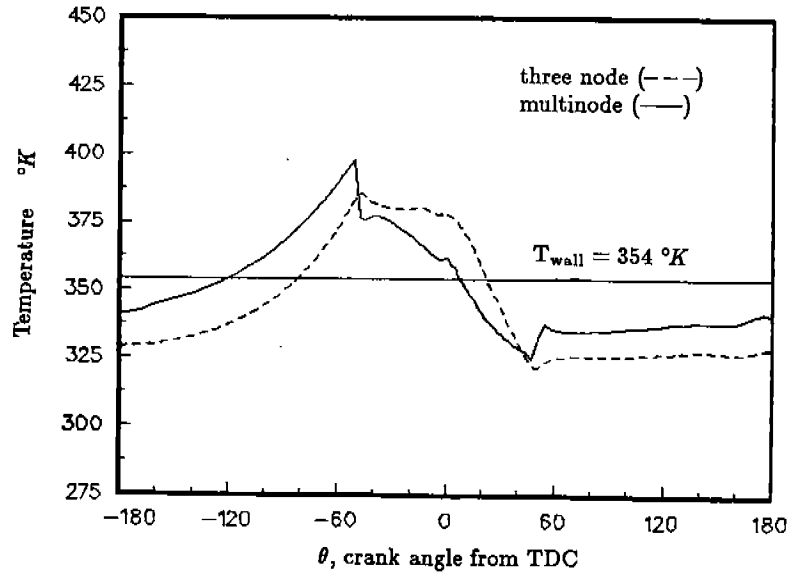

Figure 4. Comparison of instantaneous cylinder gas temperatures calculated by the three node and multinode models.

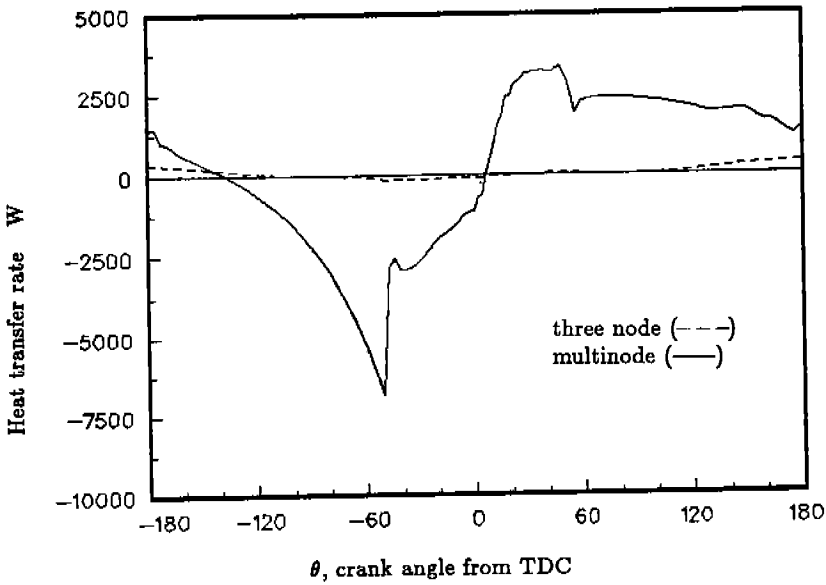

Figure 5. Comparison of instantaneous heat transfer rates calculated by the three node and multinode models.

EXPERIMENTAL INVESTIGATION ON HEAT TRANSFER IN THE MANIFOLD OF REFRIGERATING COMPRESSORS*

Gu, Yian and Wu, Yezheng

Dept. of Power Machinery Engineering, Xi'an Jiaotong University, Xi'an, China

ABSTRACT

In this study, a review and discussion has been made on the research work of heat transfer in manifolds previously done. Since it is difficult to determine the heat transfer coefficients in different areas of a suction or discharge chamber by using conventional methods, the mass transfer analogy -- sublimation of naphthalene has been used to develop the heat transfer correlations for the four areas in a suction chamber. The mass transfer experiments were carried out on a model under the stable flow conditions with air as the medium. The correctness of the correlations has been verified through the measurement of the average heat transfer coefficient in the chamber. The maximum deviation of heat transfer coefficients measured from the correlations is within ±10%.

* project supported by the Science Fund of the Chinese Acadamy of Sciences